УДК 534.121.1:534.232.082.74

Y. Yakymenko, V. Pilinsky, O. Petrishev, Y. Yanovska, O. Bogdan, S. Zelenskyy
National Technical University of Ukraine “KPI”, Research Institute “Applied Electronics”

MEMS DISK BANDPASS FILTER MATHEMATICAL MODEL

© Yakymenko Y., Pilinsky V., Petrishev O., Yanovska Y., Bogdan O., Zelenskyy S., 2010

Подано математичну модель МЕМС смугового п’єзофільтра (ПФ), побудованого на дисковій конструкції, що працює на радіальних коливаннях. Проведено дослідження частотної характеристики смугового ПФ від його геометричних параметрів, матеріалу та втрат у ньому. Отримані результати можна використати під час подальшого проектування МЕМС пристроїв.

In this paper main characteristics of a piezoceramic bandwidth filter that is used radial oscillations for its work calculation method is proposed. Also there are considered influence of next parameters on its frequency characteristic: distance to second electrode, first electrode width and electric load value. MEMS bandwidth filter designing are given.

Introduction. Because of their simple configuration and good electromechanical performance, piezoelectric elements are widely used in mobile communication system [1, 2, 3]. It has led to demand for high-performance band pass filters operating in the microwave range. This demands new method of these devices designing methods which express its accurate operation description.

Equivalent circuit method is widely used for piezoelectric filter characteristic modeling [3]. But it can not be properly used for this class of devices without device deflective state analyses, because in this method base this analysis was used [4]. That is why we need new methods for piezoelectric devises operation analysis.

In this paper the modeling method considering vibration of thing disc is presented. The vibration analysis is based on the electro elastic theory for piezoelectric disk, the Maxwell equation, resonator geometry consideration.

Radial oscillation of thing piezoceramic disc excited from the second electrode. Fig. 1 shows geomantic configuration of a thin disk with the radius R, thickness h with ring electrodes on a region $R_2 - l \le \rho \le R_2 + l$. The cylindrical coordinates (ρ, ϑ, z) with the origin in the center of the disk are used.

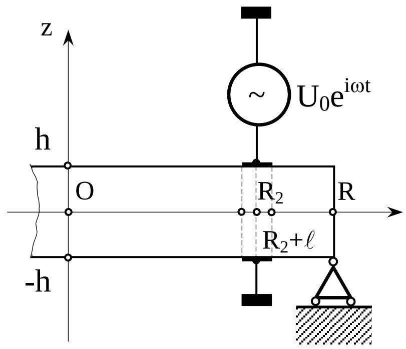

Fig. 1. Disk excitation from ring electrode

Lviv Polytechnic National University Institutional Repository http://ena.lp.edu.ua

The piezoceramic disk is polarized in the thickness direction. The excitation of the disk with external generator that generates input voltage. Analyses of the disk deflected state was provided on the base of method proposed in [5].

For disk deflective mode analyses all disk where divided into 3 region (see Fig.1): region I ($0 \le \rho \le R_2 - l, -h \le z \le h$), region II $\left(R_2 - l \le \rho \le R_2 + l, -h \le z \le h\right)$ and region III $\left(R_2 + l \le \rho \le R, -h \le z \le h\right)$. Stresses and strains in the first region are:

$$u_\rho^{(1)}(\rho) = A_1 J_1(\gamma_2 \rho), \tag{1}$$

$$\sigma_\rho^{(1)}(\rho) = c_{11}^{*} \gamma_2 A_1 (J_0(\gamma_2 \rho) + \frac{\varsigma_2 - 1}{\gamma_2 \rho} J_1(\gamma_2 \rho)), \tag{2}$$

where $u_\rho^{(1)}$ – radial strains of piezoceramic particles in region; $\sigma_\rho^{(1)}(\rho)$ – mechanical stresses in the first region; $À_1$ – constant which has to be defined; $J_n(\gamma_2 \rho)$ – n-order Bessel function; $\gamma_2^2 = \omega^2 \rho_0 \big/ c_{11}^{*}$ – wave number; ρ_0 – material density; ω – source frequency; $\varsigma_2 = c_{12}^{*} \big/ c_{11}^{*}$; $ñ_{11}^{*} = ñ_{11} + \left(\tilde{e}_{31}\right)^2 \big/ \chi_3^\sigma$; $ñ_{12}^{*} = ñ_{12} + \left(\tilde{e}_{31}\right)^2 \big/ \chi_3^\sigma$; $c_{11} = c_{11}^E - (c_{13}^E)^2 / c_{33}^E$; $c_{12} = c_{12}^E - (c_{13}^E)^2 / c_{33}^E$; $\chi_3^\sigma = \chi_3^\varepsilon \left(1 + \frac{e_{33}^2}{\chi_3^\varepsilon c_{33}^E}\right)$; χ_{ij}^ε – dielectric matrix element; $\tilde{e}_{31} = (c_{13}^E e_{33}) / c_{33}^E - e_{31}$; $e_{k\alpha}$ – piezoelectric stress matrix element; $ñ_{\alpha\beta}^E$ – stiffness matrix element.

In the second region electric field are $E_z^{(2)} = -\tilde{e}_{31} U_{in} / (2h)$. So stresses and strains in this region are:

$$u_\rho^{(2)}(\rho) = A_2 J_1(\gamma_1 \rho) + A_3 N_1(\gamma_1 \rho), \tag{3}$$

$$\begin{aligned} \sigma_\rho^{(2)}(\rho) = c_{11} \gamma_1 (A_2 (J_0(\gamma_1 \rho) + \frac{\varsigma - 1}{\gamma_1 \rho} J_1(\gamma_1 \rho)) + \\ + A_3 (N_0(\gamma_1 \rho) + \frac{\varsigma - 1}{\gamma_1 \rho} N_1(\gamma_1 \rho)) - \frac{\tilde{e}_{31} U_0}{2h \gamma_1 c_{11}}) \end{aligned}, \tag{4}$$

where A_2, A_3 – constants which have to be defined; $\varsigma = c_{12} \big/ c_{11}$; $N_n(\gamma_1 \rho)$ – Neumann function of the n-order; $\gamma_1^2 = \omega^2 \rho_0 / c_{11}$.

Stresses and strains in the third region are:

$$u_\rho^{(3)}(\rho) = A_4 J_1(\gamma_2 \rho) + A_5 N_1(\gamma_2 \rho), \tag{5}$$

$$\begin{aligned} \sigma_\rho^{(3)}(\rho) = c_{11}^{*} \gamma_2 (A_4 (J_0(\gamma_2 \rho) + \frac{\varsigma_2 - 1}{\gamma_2 \rho} J_1(\gamma_2 \rho)) + \\ + A_5 (N_0(\gamma_2 \rho) + \frac{\varsigma_2 - 1}{\gamma_2 \rho} N_1(\gamma_2 \rho))) \end{aligned}. \tag{6}$$

Equations (1), (2), (3), (4), (5) and (6) describe the deflective. Constants A_1, A_2, A_3, A_4, A_5 are defined considering dynamic balance on the boundaries. So that we have following boundary conditions:

$$u_\rho^{(1)}(R_2 - l) - u_\rho^{(2)}(R_2 - l) = 0, \tag{7}$$

$$\sigma_{\rho\rho}^{(1)}(R_2 - l) - \sigma_{\rho\rho}^{(2)}(R_2 - l) = 0, \tag{8}$$

$$u_\rho^{(2)}(R_2 + l) - u_\rho^{(3)}(R_2 + l) = 0, \tag{9}$$

$$\sigma_{\rho\rho}^{(2)}(R_2 + l) - \sigma_{\rho\rho}^{(3)}(R_2 + l) = 0, \tag{10}$$

$$\sigma_{\rho\rho}^{(3)}(R) = 0. \tag{11}$$

Lviv Polytechnic National University Institutional Repository http://ena.lp.edu.ua

Substitution of (1), (2), (3), (4), (5) and (6) in conditions (7)-(11) gives system of equations:

$$m_{ij}A_j^* = P_j, \; i, j = 1,2,3,4,5, \tag{12}$$

where $m_{11} = J_1(\gamma_2(R_2 - l))$; $m_{12} = -J_1(\gamma_2(R_2 - l))$; $m_{13} = -N_1(\gamma_2(R_2 - l))$; $m_{14} = m_{15} = 0$;
$A_j^*(j = 1,2,3,4,5)$ – dimensionless coefficients,

$$A_j = \left[\tilde{e}_{31}U_0 / (2h\gamma_1 c_{11})\right] A_j^*; \; P_1 = 0; \; m_{21} = \frac{c_{11}^*\gamma_2}{c_{11}\gamma_1}\left(J_0(\gamma_2(R_2 - l)) + \frac{\varsigma_2 - 1}{\gamma_2(R_2 - l)} J_1(\gamma_2(R_2 - l))\right);$$

$$m_{22} = -\left(J_0(\gamma_1(R_2 - l)) + \frac{\varsigma_1 - 1}{\gamma_1(R_2 - l)} J_1(\gamma_1(R_2 - l))\right); \; m_{23} = -\left(N_0(\gamma_1(R_2 - l)) + \frac{\varsigma_1 - 1}{\gamma_1(R_2 - l)} N_1(\gamma_2(R_2 - l))\right);$$

$$m_{24} = m_{25} = 0; \; P_2 = -1; \; m_{31} = 0; \; m_{32} = J_1(\gamma_1(R_2 + l)); \; m_{33} = N_1(\gamma_1(R_2 + l)); \; m_{34} = J_1(\gamma_2(R_2 + l));$$

$$m_{35} = N_1(\gamma_2(R_2 + l)); \; P_3 = 0; \; m_{41} = 0; \; m_{42} = J_0(\gamma_1(R_2 + l)) + \frac{\varsigma_1 - 1}{\gamma_1(R_2 + l)} J_1(\gamma_1(R_2 + l));$$

$$m_{43} = N_0(\gamma_1(R_2 + l)) + \frac{\varsigma_1 - 1}{\gamma_1(R_2 + l)} N_1(\gamma_2(R_2 + l));$$

$$m_{44} = -\frac{c_{11}^*\gamma_2}{c_{11}\gamma_1}\left(J_0(\gamma_2(R_2 + l)) + \frac{\varsigma_2 - 1}{\gamma_2(R_2 + l)} J_1(\gamma_2(R_2 + l))\right);$$

$$m_{45} = -\frac{c_{11}^*\gamma_2}{c_{11}\gamma_1}\left(N_0(\gamma_2(R_2 + l)) + \frac{\varsigma_2 - 1}{\gamma_2(R_2 + l)} N_1(\gamma_2(R_2 + l))\right); \; P_4 = 1; \; m_{51} = m_{52} = m_{53} = 0;$$

$$m_{54} = \frac{c_{11}^*\gamma_2}{c_{11}\gamma_1}\left(J_0(\gamma_2 R) + \frac{\varsigma_2 - 1}{\gamma_2 R} J_1(\gamma_2 R)\right); \; m_{55} = \frac{c_{11}^*\gamma_2}{c_{11}\gamma_1}\left(N_0(\gamma_2 R) + \frac{\varsigma_2 - 1}{\gamma_2 R} N_1(\gamma_2 R)\right); \; P_5 = 0$$

Principal determinant Δ_0 of the system of equations (12) if a function of dimensionless frequency γ_1. If the determinant is equal to 0 we have value of resonant frequencies. So we have equation:

$$\Delta_0 = \begin{vmatrix} m_{11} & m_{12} & m_{13} & 0 & 0 \\ m_{21} & m_{22} & m_{23} & 0 & 0 \\ 0 & m_{32} & m_{33} & m_{34} & m_{35} \\ 0 & m_{42} & m_{43} & m_{44} & m_{45} \\ 0 & 0 & 0 & m_{54} & m_{55} \end{vmatrix} = 0 \tag{13}$$

Roots of this equation are resonant frequency value. Values of 3 first resonant frequencies of PZT-19 disk for different configuration of the second electrodes are given in the table 1. Value of second electrode considered 0.05.

Bandpass MEMS filter frequency characteristic calculation. Calculation of the frequency characteristic of piezoceramic band pass filter is provided for model shown in Fig. 2. Disk excitation is provided by ring electrode and oscillation reception by central electrode.

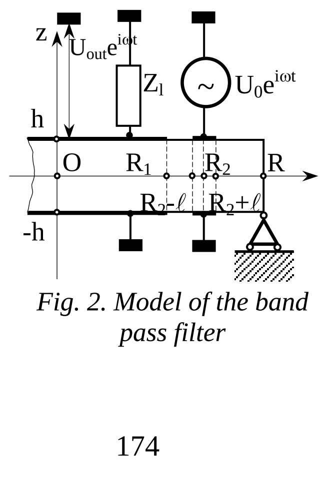

Fig. 2. Model of the band pass filter

Lviv Polytechnic National University Institutional Repository http://ena.lp.edu.ua

Disc deformation charges first region of disc ($0 \le \rho \le R_1$), covered with first electrode, and creates current through the load $Ie^{i\omega t}$ (where I - current amplitude). So voltage on load will be $U_{out}e^{i\omega t}$.

Table 1

Resonant frequency values from the second electrode position

R_2 / R	1 mode	2 mode	3 mode
0.05	2.362827	5.981881	9.449542
0.10	2.352254	5.936221	9.393028
0.15	2.342542	5.914314	9.421066
0.20	2.333980	5.916498	9.492921
0.25	2.326829	5.937971	9.555971
0.30	2.321190	5.970816	9.562454
0.35	2.317217	6.005178	9.502306
0.40	2.314898	6.030460	9.420109
0.45	2.314298	6.038286	9.374444
0.50	2.315220	6.025760	9.393945
0.55	2.317680	5.997005	9.465781
0.60	2.321488	5.961011	9.542326
0.65	2.326430	5.927965	9.568080
0.70	2.332301	5.906435	9.525917
0.75	2.338785	5.901920	9.448688
0.80	2.345546	5.916239	9.385749
0.85	2.352232	5.946532	9.376011
0.90	2.358509	5.984615	9.432042
0.95	2.364021	6.018435	9.519089

The output voltage amplitude is:

$$U_{out} = IZ_{\acute{\imath}} \ . \tag{14}$$

Current I amplitude is:

$$I = -i\omega q \tag{15}$$

As value of first electrode charge q is:

$$q = 2\pi \int_0^{R_1} \rho D_z^{(1)}(\rho) d\rho \ , \tag{16}$$

Where $D_z^{(1)}(\rho)$ is axial component of the electric flux density vector in region №1 ($0 \le \rho \le R_1, 0 \le \vartheta \le 2\pi, -h \le z \le h$). Then this value is:

$$D_z^{(1)}(\rho) = -\tilde{e}_{31}\left(\frac{\partial u_\rho^{(1)}}{\partial \rho} + \frac{u_\rho^{(1)}}{\rho}\right) - \frac{\chi_3^\sigma U_{out}}{2h} \tag{17}$$

Next we substitute (17) into electric charge definition equation (16) and providing integration by parts we receive:

$$q = -\frac{4hC_2\tilde{e}_{31}}{\chi_3^\sigma}\varepsilon_v - C_2 U_{out} \ , \tag{18}$$

where C_2 – static electrical capacitance of the first electrodes and its value $C_2 = \pi R_1^2 \chi_3^\sigma / (2h)$, ε_v – relative volume changing in the first region. Volume deformation ε_v is defined by the equation:

$$\varepsilon_v = \frac{u_\rho^{(1)}(R_1) - u_\rho^{(1)}(0)}{R_1} \ .$$

Lviv Polytechnic National University Institutional Repository http://ena.lp.edu.ua

Substituting q in (3.2) and (3.1) we receive:

$$U_{out} = -\frac{i\omega\tau_e}{1+i\omega\tau_e} \cdot \frac{4h\tilde{e}_{31}}{\chi_3^{\sigma}} \varepsilon_V, \qquad (19)$$

where $\tau_e = \tilde{N}_2 Z_í$ – is time constant of first electrodes circuit.

Thus output voltage U_{out} is defined by the value of strains under first electrodes $u_\rho^{(1)}$. Calculation of $u_\rho^{(1)}$ is provided with analyses of the piezoceramic disk deflected states.

Strains are calculated for four regions of the disk.

Region №1 is situated in the volume ($0 \le \rho \le R_1$, $0 \le \vartheta \le 2\pi, -h \le z \le h$) covered with central electrodes. The electric field in this region are $E_z^{(1)} = -\tilde{e}_{31} U_{out} / (2h)$. Strains $u_\rho^{(1)}$ and stresses $\sigma_{\rho\rho}^{(1)}$ in this region are:

$$u_\rho^{(1)} = A_1 J_1(\gamma_1 \rho), \qquad (20)$$

$$\sigma_{\rho\rho}^{(1)} = c_{11} \frac{\partial u_\rho^{(1)}}{\partial \rho} + c_{12} \frac{u_\rho^{(1)}}{\rho} + \frac{2i\omega\tau_e}{1+i\omega\tau_e} \tilde{n}_{11} k_{31}^2 \varepsilon_v, \qquad (21)$$

Normal stress $\sigma_{\vartheta\vartheta}^{(1)}$ is defined from the state equations (see (1.4) in [5]) similarly to (21) by the equation:

$$\sigma_{\vartheta\vartheta}^{(1)} = c_{11} \frac{\partial u_\rho^{(1)}}{\partial \rho} + c_{12} \frac{u_\rho^{(1)}}{\rho} + \frac{2i\omega\tau_e}{1+i\omega\tau_e} \tilde{n}_{11} k_{31}^2 \varepsilon_v .$$

Region №2 is situated in volume ($R_1 \le \rho \le R_2 - l$, $0 \le \vartheta \le 2\pi, -h \le z \le h$). The stresses $\sigma_{\rho\rho}^{(2)}$ and strains $u_\rho^{(2)}$ in this region are following:

$$u_\rho^{(2)} = A_2 J_1(\gamma_2 \rho) + A_3 N_1(\gamma_2 \rho), \qquad (22)$$

$$\sigma_{\rho\rho}^{(2)} = c_{11}^* \frac{\partial u_\rho^{(2)}}{\partial \rho} + c_{12}^* \frac{u_\rho^{(2)}}{\rho}. \qquad (23)$$

Region №3 is covered with ring electrodes. The radial stress in this region $\sigma_{\rho\rho}^{(3)}$ is defined by the following equation:

$$\sigma_{\rho\rho}^{(3)} = c_{11} \frac{\partial u_\rho^{(3)}}{\partial \rho} + c_{12} \frac{u_\rho^{(3)}}{\rho} - \frac{\tilde{e}_{31} U_0}{2h}, \qquad (24)$$

Substitution of the values $\sigma_{\vartheta\vartheta}^{(3)}$ and $\sigma_{\rho\rho}^{(3)}$ in the equations of the sustained radial vibrations [5] gives radial strains values $u_\rho^{(3)}$:

$$u_\rho^{(3)} = A_4 J_1(\gamma_1 \rho) + A_5 N_1(\gamma_1 \rho), \qquad (25)$$

Region №4 is in the volume ($R_2 + l \le \rho \le R$, $0 \le \vartheta \le 2\pi, -h \le z \le h$) strains $u_\rho^{(4)}$ and stresses $\sigma_{\rho\rho}^{(4)}$ are defined be the following expressions:

$$u_\rho^{(4)} = A_6 J_1(\gamma_2 \rho) + A_7 N_1(\gamma_2 \rho), \qquad (26)$$

$$\sigma_{\rho\rho}^{(4)} = c_{11}^* \frac{\partial u_\rho^{(4)}}{\partial \rho} + c_{12}^* \frac{u_\rho^{(4)}}{\rho}. \qquad (27)$$

Lviv Polytechnic National University Institutional Repository http://ena.lp.edu.ua

Seven unknown constants $A_1,\ldots,A_7$, that are used for the disk deflective state description for different regions, are defined of conditions of the dynamic and cinematic coupling in the boundaries of regions. These boundary conditions are stated by the following equations:

$$u_\rho^{(1)}(R_1)-u_\rho^{(2)}(R_1)=0, \tag{28}$$

$$\sigma_{\rho\rho}^{(1)}(R_1)-\sigma_{\rho\rho}^{(2)}(R_1)=0, \tag{29}$$

$$u_\rho^{(2)}(R_2-l)-u_\rho^{(3)}(R_2-l)=0, \tag{30}$$

$$\sigma_{\rho\rho}^{(2)}(R_2-l)-\sigma_{\rho\rho}^{(3)}(R_2-l)=0, \tag{31}$$

$$u_\rho^{(3)}(R_2+l)-u_\rho^{(4)}(R_2+l)=0, \tag{32}$$

$$\sigma_{\rho\rho}^{(3)}(R_2+l)-\sigma_{\rho\rho}^{(4)}(R_2+l)=0, \tag{33}$$

$$\sigma_{\rho\rho}^{(4)}(R)=0. \tag{34}$$

Substitution of (20) – (26) into conditions (28) – (34) forms inhomogeneous linear system of equations. Solution of this system defines values of unknown constants $A_1,\ldots,A_7$.

General presentation of this system is:

$$A_j^* m_{ij}=P_i;\ i,j=1,\ldots,7, \tag{35}$$

where A_j^* – are dimensionless constants, that defines constants $A_j\ (j=1,\ldots,7)$ as $A_j=\left[\tilde{e}_{31}U_0/\left(2h\gamma_1 c_{11}\right)\right]A_j^*$; m_{ij} – dimensionless coefficients; P_i – column matrix of the right part $P_4=P_6=1$, other values are $P_i=0$. So we receive matrix coefficients values:

$$m_{11}=J_1(\gamma_1R_1);\ m_{12}=-J_1(\gamma_2R_1);\ m_{13}=-N_1(\gamma_2R_1);\ m_{14}=m_{15}=m_{16}=m_{17}=0;\ g=\frac{i\omega\tau_e}{1+i\omega\tau_e};$$

$$m_{21}=J_0(\gamma_1R_1)+\frac{\varsigma_1-1+2gk_{31}^2}{\gamma_1R_1}J_1(\gamma_1R_1);\ m_{22}=-\frac{c_{11}^*\gamma_2}{c_{11}\gamma_1}\left(J_0(\gamma_2R_1)+\frac{\varsigma_2-1}{\gamma_2R_1}J_1(\gamma_2R_1)\right);$$

$$m_{23}=-\frac{c_{11}^*\gamma_2}{c_{11}\gamma_1}\left(N_0(\gamma_2R_1)+\frac{\varsigma_2-1}{\gamma_2R_1}N_1(\gamma_2R_1)\right);\ m_{24}=m_{25}=m_{26}=m_{27}=0;\ m_{31}=0;\ m_{32}=J_1(\gamma_2(R_2-l));$$

$$m_{33}=N_1(\gamma_2(R_2-l));\ m_{34}=-J_1(\gamma_1(R_2-l));\ m_{35}=-N_1(\gamma_1(R_2-l));\ m_{36}=m_{37}=0;$$

$$m_{41}=0;\ m_{42}=\frac{c_{11}^*\gamma_2}{c_{11}\gamma_1}\left[J_0(\gamma_2(R_2-l))+\frac{\varsigma_2-1}{\gamma_2(R_2-l)}J_1(\gamma_2(R_2-l))\right];$$

$$m_{43}=\frac{c_{11}^*\gamma_2}{c_{11}\gamma_1}\left[N_0(\gamma_2(R_2-l))+\frac{\varsigma_2-1}{\gamma_2(R_2-l)}N_1(\gamma_2(R_2-l))\right];\ m_{45}=-\left(J_0(\gamma_1(R_2-l))+\frac{\varsigma_1-1}{\gamma_1(R_2-l)}J_1(\gamma_1(R_2-l))\right);$$

$$m_{46}=-\left(N_0(\gamma_1(R_2-l))+\frac{\varsigma_1-1}{\gamma_1(R_2-l)}N_1(\gamma_1(R_2-l))\right);\ m_{46}=m_{47}=0;\ m_{51}=m_{52}=m_{53}=0;\ m_{54}=J_1(\gamma_1(R_2+l));$$

$$m_{55}=N_1(\gamma_1(R_2+l));\ m_{56}=-J_1(\gamma_2(R_2+l));\ m_{57}=-N_1(\gamma_2(R_2+l));\ m_{61}=m_{62}=m_{63}=0;$$

$$m_{64}=J_0(\gamma_1(R_2+l))+\frac{\varsigma_1-1}{\gamma_1(R_2+l)}J_1(\gamma_1(R_2+l));\ m_{65}=N_0(\gamma_1(R_2+l))+\frac{\varsigma_1-1}{\gamma_1(R_2+l)}N_1(\gamma_1(R_2+l));$$

$$m_{66}=-\frac{c_{11}^*\gamma_2}{c_{11}\gamma_1}\left(J_0(\gamma_2(R_2+l))+\frac{\varsigma_2-1}{\gamma_2(R_2+l)}J_1(\gamma_2(R_2+l))\right);$$

$$m_{67}=-\frac{c_{11}^*\gamma_2}{c_{11}\gamma_1}\left[N_0(\gamma_2(R_2+l))+\frac{\varsigma_2-1}{\gamma_2(R_2+l)}N_1(\gamma_2(R_2+l))\right];\ m_{71}=m_{72}=m_{73}=m_{74}=m_{75}=0;$$

$$m_{76}=J_0(\gamma_2R)+\frac{\varsigma_2-1}{\gamma_2R}J_1(\gamma_2R);\ m_{77}=N_0(\gamma_2R)+\frac{\varsigma_2-1}{\gamma_2R}N_1(\gamma_2R).$$

Lviv Polytechnic National University Institutional Repository http://ena.lp.edu.ua

The constant A_1, which value defines strains $u_\rho^{(1)}(\rho)$ and output voltage U_{out}, is:

$$A_1 = \frac{\tilde{e}_{31}U_0}{2h\gamma_1 c_{11}}\frac{(\Delta_{41}-\Delta_{61})}{\Delta_{\grave{o}}}, \tag{36}$$

where $\Delta_{\grave{o}}$ – is the determinant of the system of equation (35), and Δ_{k1} $(k = 4,6)$ are algebraic adjunct of this system.

Substitution of (36) into (19) defines output voltage U_{out}. Its value is:

$$U_{out} = -\,i\omega U_0 \frac{2k_{31}^2}{\gamma_1 R_1}\frac{\tau_e\left(\Delta_{41}-\Delta_{61}\right)J(\gamma_1 R_1)}{(1+i\omega\tau_e)\Delta_{\grave{o}}},$$

From there frequency characteristic of piezoceramic bandpass filter shown in fig. 3.1 is:

$$k(\omega) = \frac{U_{out}}{U_0} = -\,i\omega \frac{2k_{31}^2}{\gamma_1 R_1}\frac{\tau_e\left(\Delta_{41}-\Delta_{61}\right)J(\gamma_1 R_1)}{(1+i\omega\tau_e)\Delta_{\grave{o}}}, \tag{37}$$

On the next stage of the research we analyze frequency characteristic dependence from different disk geometric parameters. Material of the disk is PZT 19, its parameters are following: $\tilde{n}_{11}^{\AA} = \tilde{n}_{22}^{\AA} =$ 109 GPa; $\tilde{n}_{33}^{\AA} = 93$ GPa; $\tilde{n}_{12}^{\AA} = \tilde{n}_{13}^{\AA} = 54$ GPa; $\tilde{n}_{23}^{\AA} = 61$ GPa; $\rho_0 = 7400$ kg/m^3; $\mathring{a}_{31} = \mathring{a}_{32} = -4{,}9$ C/m^2; $\mathring{a}_{33} = 14{,}9$ C/m^2; $\chi_1^\varepsilon = \chi_2^\varepsilon = 820\chi_0$; $\chi_1^\varepsilon = \chi_2^\varepsilon = 820\chi_0$; $\chi_0 = 8{,}85\cdot 10^{-12}$ F/m; $Q = 80$.

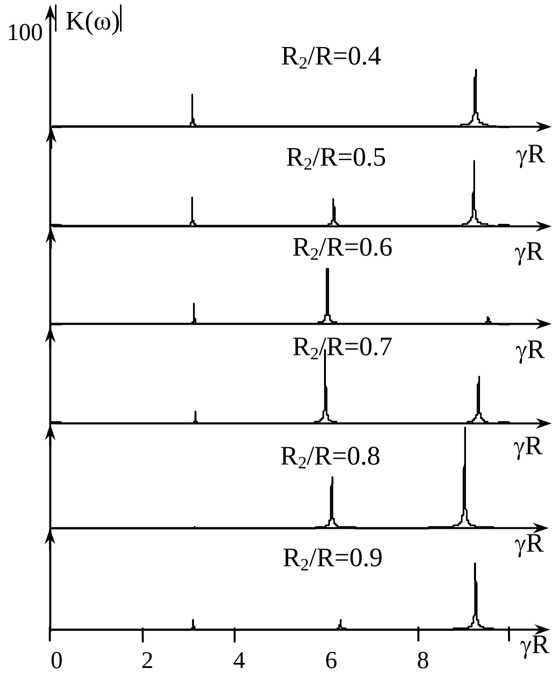

Fig. 3. Frequency characteristics for different values of R_1/R

In Fig.3 is shown dependence of the frequency characteristic from the value of central electrode R_1/R. Other geometric disk: $R_2/R = 0{,}7; l/R = 0{,}1; \tau_e/\tau = 1;$ $\tau_0 = R/\nu_r; \nu_r = \sqrt{c_{11}/\rho_0}$.

We see that value of the first electrode is control intensity of the output voltage.

In Fig.4 is shown dependence of the frequency characteristic from the position of the ring electrode R_2/R ,other disk parameters: $R_1/R = 0{,}1; l/R = 0{,}1; \tau_e/\tau = 1$, $\tau_0 = R/\nu_r; \nu_r = \sqrt{c_{11}/\rho_0}$.

Position of the second electrode R_2/R controlling values of the resonance frequencies, intensity of resonance characteristic.

Lviv Polytechnic National University Institutional Repository http://ena.lp.edu.ua

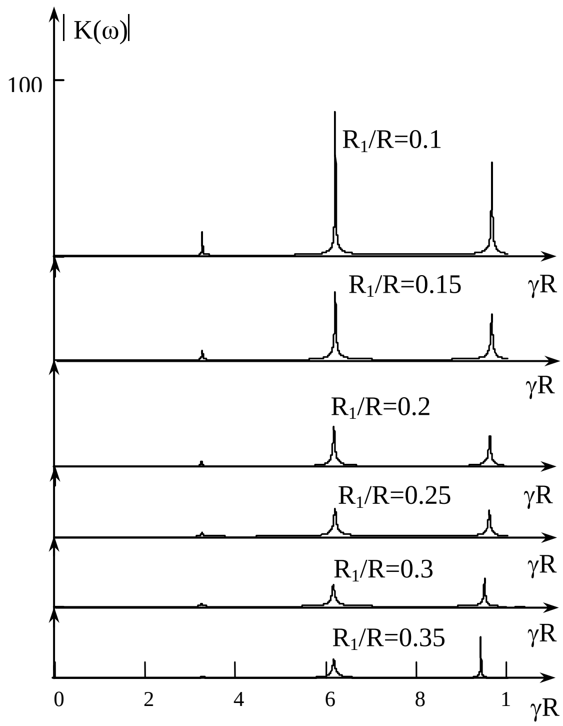

Fig. 4. Frequency characteristics from the positions of ring electrode R_2-ℓ

In Fig.5 is shown frequency characteristic dependence from the value of the second electrode l/R, other disk parameters: $R_1/R = 0{,}1; R_2/R = 0{,}7; \tau_e/\tau = 1$, $\tau_0 = R/\nu_r; \nu_r = \sqrt{c_{11}/\rho_0}$. Received results show that second electrode value is influence mainly on the characteristic magnitudes.

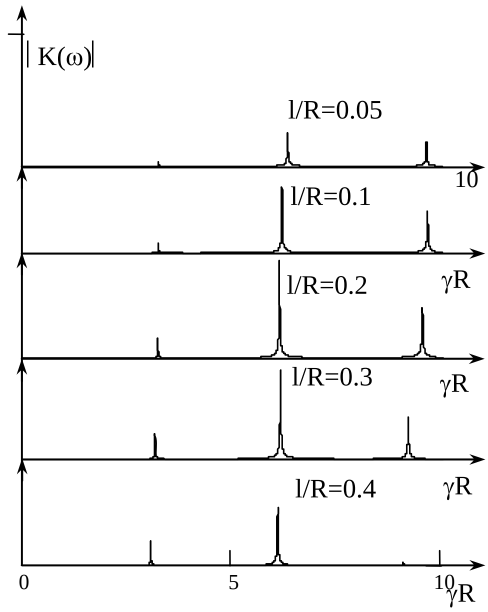

Fig. 5. Frequency characteristics for different values of the second

Conclusion. In this paper is proposed method of the calculation of MEMS bandpass filtel frequency characteristic considering its geometric parameters and material. The analyses where provided considering deflective mode in the disk. It is supposeв that disk is operating in radial mode.

Lviv Polytechnic National University Institutional Repository http://ena.lp.edu.ua

Analyses provided shows that controlling firs and second electrode value and second electrode position we controlling frequency characteristic parameters.

1. Варадан В., Виной К., Джозе К.ВЧ МЭМС и их применение. – М.: Техносфера, 2004. – 528 с. 2. Ruby R. Micromachined cellular filters, Microwave Symposium Digest // IEEE MTT-S International, pp. 370-377, 1996. 3. Pedro de Paco, Oscar Menendez "Equivalent circuit modeling of coupled resonator filters", IEEE transactions on Ultrasonic, Ferroelectrics and Frequency control, vol. 53, No 9, pp. 2030–2037, sept. 2008. 4. Cady W. Piezoelectricity. An introduction to the theory and application of electro-mechanical phenomena in crystal, first edition. – New York–London, 1946. – 717. 5. Богдан А.В., Петрищев О.Н., Якименко Ю.И., Яновская Ю.Ю. Исследование характеристик пьезоэлектрического трансформатора на основе радиальных колебаний тонких пьезокерамических дисков // Электроника и связь: Тематический выпуск "Проблемы электроники". – 2009. – Ч.1 – С.269–274.

УДК 621.395.7

М.Й. Павликевич
Національний університет "Львівська політехніка",
кафедра

БАЗОВА МАТЕМАТИЧНА МОДЕЛЬ БАГАТОПРОВІДНОЇ ЛІНІЇ У КВАЗІСТАЦІОНАРНОМУ НАБЛИЖЕННІ

© Павликевич М.Й., 2010

Наведено основні розрахункові співвідношення для математичної моделі багатопровідної лінії з паралельними круглими провідниками в круглій діелектричній ізоляції над провідною площиною. Первинні параметри лінії отримані у квазістаціонарному наближенні.

This article presents the model a multiconductor transmission line with parallel round wires surrounded by a dielectric insulation over ground plane. Primary parameters of a line are obtained in quasi-stationary approximation.

Вступ. Вивчення властивостей багатопровідних передавальних ліній важливе для їхнього ефективного використання в сучасних широкосмугових технологіях, зокрема, у технології Ethernet зі швидкостями пересилання понад 10 Гб/с. У більшості публікацій для теоретичних досліджень використовується апарат моделювання на основі теорії кіл із зосередженими параметрами (наприклад, PSPICE), недостатньо адекватний для випадків, коли довжина відрізка лінії порівняльна або перевищує довжину хвилі. У цій роботі для досліджень запропоновано використання базової математичної моделі регулярної багатопровідної лінії, утвореної системою паралельних циліндричних провідників у циліндричній діелектричній ізоляції, розташованих над провідною площиною так, що осі провідників паралельні між собою та до екрана (рис. 1). Модель побудована для наближення квазі-Т-хвиль з використанням апарата теорії багатопровідних ліній з розподіленими параметрами. Обчислення первинних параметрів лінії здійснено у квазістаціонарному наближенні, а для розрахунків передавальних властивостей застосовано апарат теорії багатополюсників у класичному та хвильовому варіантах. Модель називається базовою, оскільки на її основі моделювання можна поширити на лінії різноманітної конфігурації, зокрема на нерегулярні лінії, утворені скрученими провідниками, на лінії типу «скручена пара».

Lviv Polytechnic National University Institutional Repository http://ena.lp.edu.ua